Fermi National Accelerator Laboratory

FERMILAB-Conf-94/336-E

Studies of Prompt Photon Production and Multijet Production at the Tevatron Collider

Elizabeth Buckley-Geer
The CDF Collaboration

Fermi National Accelerator Laboratory

September 1994

Published Proceedings *27th International Conference on High Energy Physics, University of Glasgow,* Glasgow, Scotland, July 20-27, 1994

Disclaimer

CDF/PUB/JET/PUBLIC/2820

FERMILAB-CONF-94/336-E

Studies of Prompt Photon production and Multijet production at the Tevatron Collider

Elizabeth Buckley-Geer

Fermi National Accelerator Laboratory
Batavia, Illinois 60510

Presented on behalf of the CDF and D0 Collaborations

Abstract

We present measurements of inclusive isolated prompt photon production in $p\bar{p}$ collisions at a center-of-mass energy of 1.8 TeV from the Fermilab experiments CDF and D0. Precision measurements of prompt photon production from CDF constrain the gluon distribution, and recent results from D0 agree with CDF and QCD predictions. We also present studies of events with up to six jets in the final state from the CDF experiment. The mass distributions and mass ratio for these events is well described by the HERWIG parton shower Monte Carlo and by leading order QCD. Finally we present studies by both CDF and D0 of events with three jets in the final state.

Published Proceedings 27th International Conference on High Energy Physics, University of Glasgow, Glasgow, Scotland, July 20-27, 1994

1. Inclusive Isolated Prompt Photon Production

Prompt photon production at the Tevatron Collider is a precision test of Quantum Chromodynamics (QCD). At lowest order the dominant production mechanism is via Compton scattering off a gluon in the initial state. This implies that prompt photons provide a way to study the gluon distribution of the proton. Typical x_T values for the photons are in the range $0.01 - 0.1$.

1.1. Data Sample and Event Selection

In order to measure prompt photons both CDF and D0 use electromagnetic (EM) calorimeters segmented into towers in $\eta - \phi$ space. The main background is from neutral mesons, π^0, η and K_S^0 in jets which are suppressed by requiring that the photon candidate be isolated. CDF requires that there be less that 2 GeV of energy in a cone of ΔR ($\Delta R = \sqrt{\Delta\eta^2 + \Delta\phi^2}$) around the photon while D0 requires that there be less than 2 GeV of energy in an annulus between $R = 0.2$ and $R = 0.4$. Additional cuts are applied to obtain the final sample, these are summarized in Table 1.

CDF had an isolation cut in the hardware trigger that allowed it to acquire more photon data at low p_T . The CDF sample for this analysis was 0.06 pb^{-1} above 6 GeV, 18 pb^{-1} above 16 GeV and 21 pb^{-1} above 50 GeV while the D0 sample was 0.005 pb^{-1} above 6 GeV, 0.022 pb^{-1} above 14 GeV and 3.86 pb^{-1} above 30 GeV.

1.2. Background subtraction methods

After all cuts the remaining background is predominantly from isolated π^0 and η mesons. The background subtraction methods for the two experiments are described separately.

1.2.1. CDF methods The CDF experiment uses two methods to subtract the neutral meson backgrounds. The *profile method* uses the transverse profile at shower maximum in the central strip chambers. The transverse profile of the shower is compared to the profile for a testbeam shower and a χ^2 is extracted. This χ^2 is larger for π^0 and η mesons than for single photons. The *conversion method* uses photon conversions occurring in the magnet coil which are then detected in the preshower detector. The probability of a π^0 and η meson converting is higher than a single photon. The efficiencies of the two methods are illustrated in figure 1 for photon candidates, simulated photons and background. The fraction of photons in the data is $f = (\epsilon - \epsilon_B)/(\epsilon_\gamma - \epsilon_B)$ where ϵ, ϵ_γ and ϵ_B are the efficiencies from the two methods for photon candidates, pure photons and pure background.

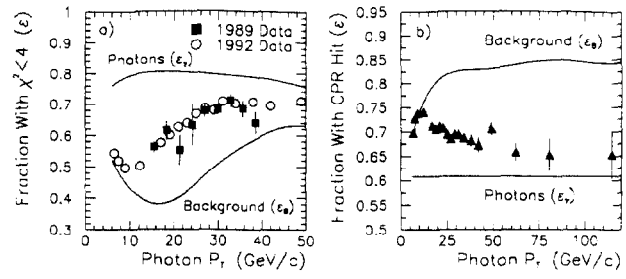

Figure 1. CDF background subtraction efficiency ϵ for photon candidates compared with simulated photons and background for a) the profile method and b) the conversion method.

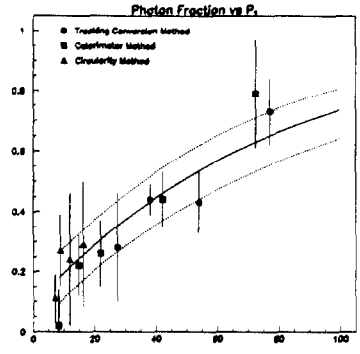

Figure 2. D0 photon fraction f for the three methods of background subtraction. The solid line is a fit and the dotted lines are the errors of the fit.

1.2.2. D0 Methods D0 uses three methods for background subtraction. Two of the methods rely on the probability that the background is more likely to convert than the signal. One expects that the calorimeter shower for a background event will start earlier that for a single photon so the ratio of energy in the first depth segment of the calorimeter is compared to the total shower energy. Conversions can also be tagged as track with twice the minimum ionizing energy using a dE/dx measurement in the Central Drift Chambers. The third method uses the asymmetry in the calorimeter showers caused by the opening angle between the two photons from a background event. This only works for low p_T photons. A functional form for the photon fraction f is extracted by fitting the three subtraction methods using the relationship above (figure 2).

1.3. Inclusive Photon Results

The differential cross-section measured by CDF is shown in fig[illegible] region they agree to within 5%. Although there is qualatative agreement between the data and the QCD prediction[1], in figure 4 we show that the data has a steeper slope at low p_T regardless of the choice of parton distribution or renormalization scale. The overall systematic uncertainty is 10% at $p_T = 16$ GeV.

Analysis Cut	CDF	D0
EM Energy/Total Energy	> 0.89	> 0.96
Neutral Cluster	No track	dE/dx separation
Shower profile	Good strip chi^2	Depth/transverse χ^2
Suppress η mesons	Extra strips < 1 GeV	
Reject cosmic rays	$\not\!\!E_T / E_T^\gamma < 0.8$	$\not\!\!E_T / E_T^\gamma < 0.5$
Good z-vertex	$\|Z_v\| < 50$ cm	
Central photon	$\|\eta\| < 0.9$	$\|\eta\| < 0.9$

Table 1. Isolated photon event selection cuts.

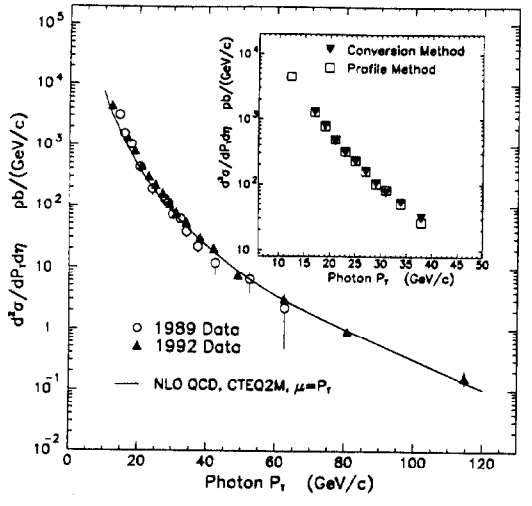

Figure 3. The isolated photon cross-section measured by CDF.

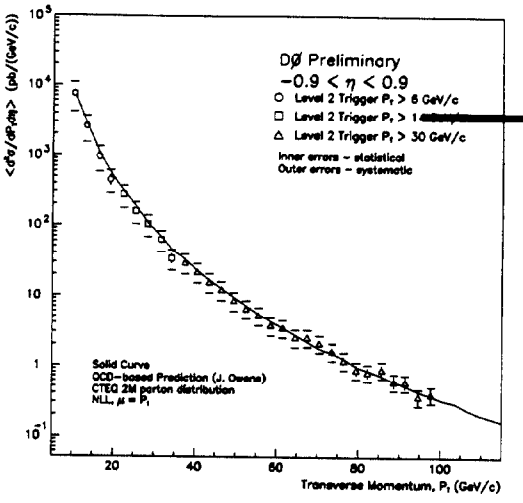

Figure 5. The isolated photon cross-section measured by D0.

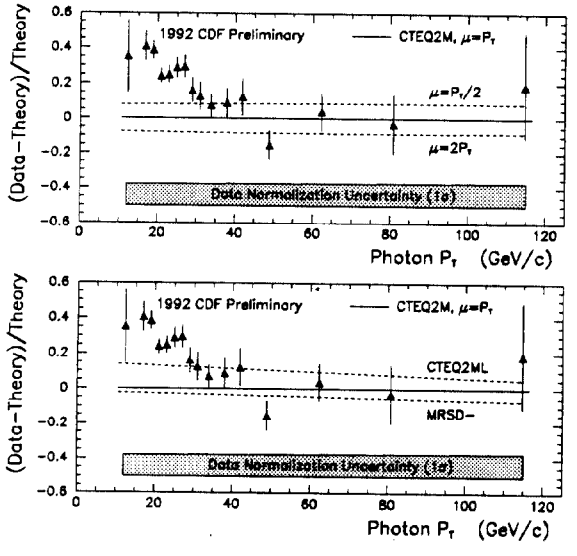

Figure 4. Comparison between data and QCD for different choices of renormalization scale and parton distributions.

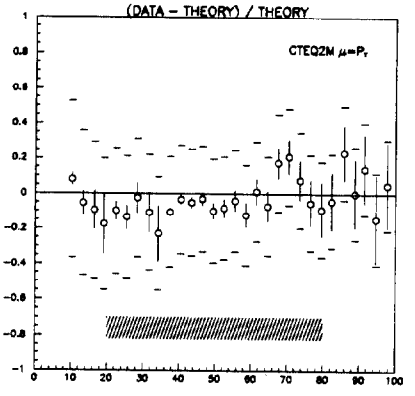

Figure 6. Comparison between data and QCD using CTEQ2M parton distributions.

The differential cross-section measured by D0 is shown in figure 5 and uses the same parameters for the QCD comparison. The linear comparison is shown in figure 6. Within the systematic errors there is good agreement between the data and the prediction.

The shaded band in figure 6 corresponds to a $\pm 12\%$ normalization uncertainty on the luminosity.

2. Multijet Production at CDF

CDF has performed a study of multijet final states (up to 10 jets were observed) using a sample of events with large total transverse energy ($\sum E_T$). The aim of the study is to compare the data to leading order QCD predictions where available, and with parton shower

Monte Carlo predictions. This is the continuation of a previous study done by CDF on event with large total transverse energy[2].

2.1. *Data Sample and Event Selection*

The events were collected using a trigger that required $\sum E_T > 175$ GeV where the sum was over all Level 2 calorimeter clusters. A software Level 3 trigger further required that $\sum E_T > 300$ GeV where the sum was over offline calorimeter clusters with $E_T > 10$ GeV.

In additions events were required to pass the following selection criteria

1 $\sum E_T > 420$ GeV where the sum is over offline calorimeter clusters with corrected $E_T > 20$ GeV (jet cone $\Delta R = 0.7$).

2 $E_{Tot} < 2000$ GeV.

3 At least one reconstructed vertex with $|z| < 60$ cm.

4 Missing E_T significance $S < 6$ ($S \equiv \not\!\!E_T/(\sum E_T)^{1/2}$).

5 No significant energy in the calorimeters that is out-of-time with the proton-antiproton collision.

This resulted in a sample of 4632 events.

2.2. *QCD Predictions*

The leading order QCD predictions were obtained using the NJETS[3] program which is a parton level calculation using $2 \to N$ matrix elements. The following parameters were used in the calculation

1 $\sum E_T$ (parton) > 420 GeV, $E_T > 20$ GeV, $|\eta| < 3.0$, $\Delta R(j,j) > 1.0$.

2 MRSD0[4] parton distributions and $Q^2 = \langle E_T(jet) \rangle$

3 The parton transverse energies were smeared using a gaussian resolution function, $\sigma_{E_T} = 0.1 E_T$ (approximately the CDF resolution function).

Predictions have been generated for $2 \to N$ where $N = 2, 3, 4, 5$. We have also used the parton shower Monte Carlo HERWIG[5] plus a full simulation of the CDF detector. We used the CTEQ1M[6] parton distributions and $Q^2 = stu/2(s^2 + t^2 + u^2)$.

The jet multiplicity distribution for the events is shown in figure 7 compared to the prediction from the HERWIG Monte Carlo. HERWIG underestimates the observed fraction of events with jet multiplicities larger that five and the discrepancy increases with increasing jet multiplicity. We suspect that this reflects a limitation of the HERWIG predictions. This effect has been observed previously in W + N-jet production[7].

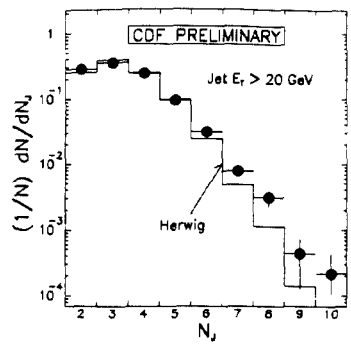

Figure 7. The jet multiplicity distribution. The jets were reconstructed with a cone size of $\Delta R = 0.7$ and the energies have been corrected.

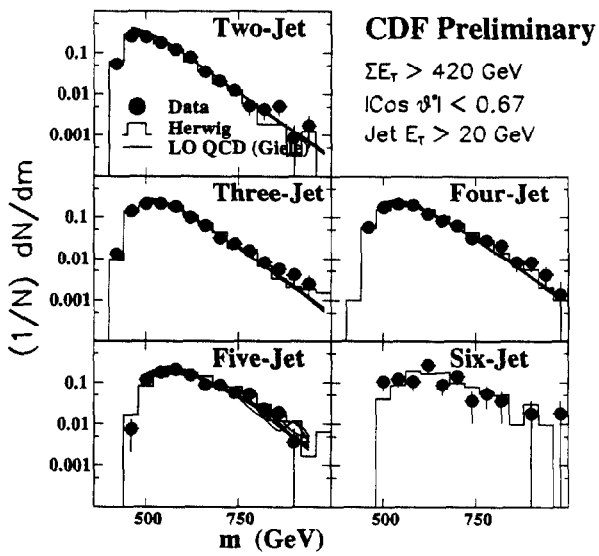

Figure 8. The multijet mass distribution. The jets were reconstructed with a cone size of $\Delta R = 0.7$ and the energies have been corrected.

2.3. *Multijet mass distributions*

In order to study the mass dependence of the events we require all events to have the center-of-mass scattering angle of the leading jet in the N-body rest-frame, $\cos\theta^* < 0.67$. This ensures that the data are fully efficient for the chosen $\sum E_T$ threshold. The mass distributions for events with jet multiplicities up to six jets are shown in figure 8. They are compared to HERWIG and to NJETS, both can be seen to give a good description of the data in the fully efficient region which is $M_{Nj} > 600$ GeV. We have studied the variation of the NJETS prediction by changing the parton distributions and the Q^2 scale. There is no change in shape although the normalization varies.

We have also studied the $N - jet/2 - jet$ ratio as a function of M_{Nj}. This is shown in figure 9. The

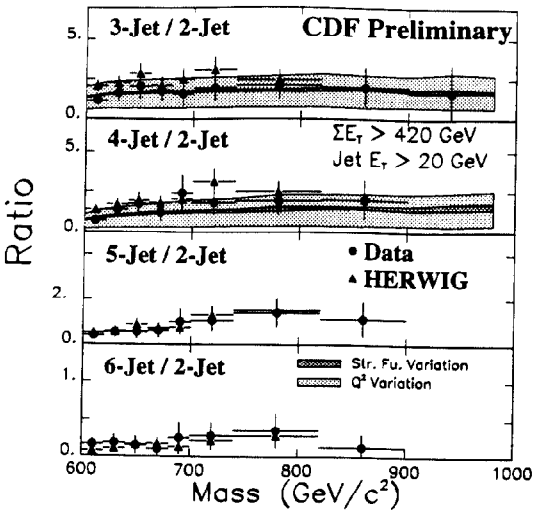

Figure 9. The $N - jet/2 - jet$ ratio as a function of M_{Nj}.

data are in reasonable agreement with the HERWIG predictions. There is some tendency for the HERWIG prediction to be high for low jet multiplicities and vice versa. The data are also well described by the range of NJETS predictions. The uncertainty due to the Q^2 scale dominates.

3. Three-jet Production

Studies of three-jet production have been performed by both CDF and D0. These studies use the same kinematic variables as previous UA1 and CDF studies [8]. These are

1 m_{3j},the three-jet mass.

2 x_3, x_4 which are the energy fractions of two leading jet(jets are ordered so that $E_3 > E_4 > E_5$) $x_i = 2E_i/\sum E_j$.

3 $\cos\theta_3^\star$, the cosine of the leading-jet scattering angle.

4 $\psi^\star$, the angle between the production plan and the three-jet plane.

The event selection cuts for both CDF and D0 are summarized in Table 2. The CDF study starts from the $\sum E_T$ sample descibed in section 2 while D0 uses an inclusive jet sample.

These cuts yield 522 events for the CDF sample and 7179 for the D0 sample which has larger angular acceptance and a lower mass cut.

In figure 10 we show the four kinematic variables described above for the CDF experiment compared to the predictions from the HERWIG Monte Carlo. The agreement is good. In figure 11 are shown the corresponding plots for D0. Here the Monte Carlo

Analysis Cut	CDF	D0
Jet E_T	$E_T > 20$ GeV	$E_T > 20$ GeV
$\|\eta\|$		< 3.0
ΔR		> 1.4
Highest E_T jet		> 60 GeV
m_{3j}	> 500 GeV	$> 250 GeV$
x_3	< 0.9	< 0.9
$\|\cos\theta_3^\star\|$	< 0.6	< 0.95
$\psi^\star$		$20° < \psi^\star < 160°$

Table 2. Three-jet event selection cuts.

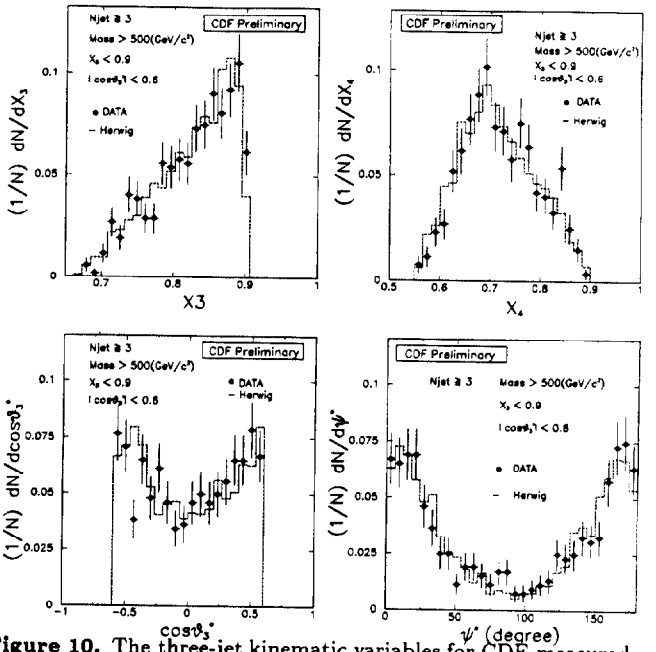

Figure 10. The three-jet kinematic variables for CDF measured at high m_{3j}.

used is NJETS with no detector simulation. Again the agreement with theory is good.

4. Conclusions

The prompt photon cross-section from CDF is in qualatative agreement with next-to-leading order QCD but has a steeper slope at low p_T . Work is currently in progress to try and include the CDF data into the CTEQ global fits. The photon cross-section from D0 is in good agreement both with next-to-leading order QCD and CDF. The multijet mass distributions are well described by HERWIG and leading order QCD in the fully efficient region, as is the $N - jet/2 - jet$ mass ratio. The high-mass three-jet events from CDF are well described by the HERWIG Monte Carlo. The D0 events cover a larger mass and angular range and are well described by leading order QCD.

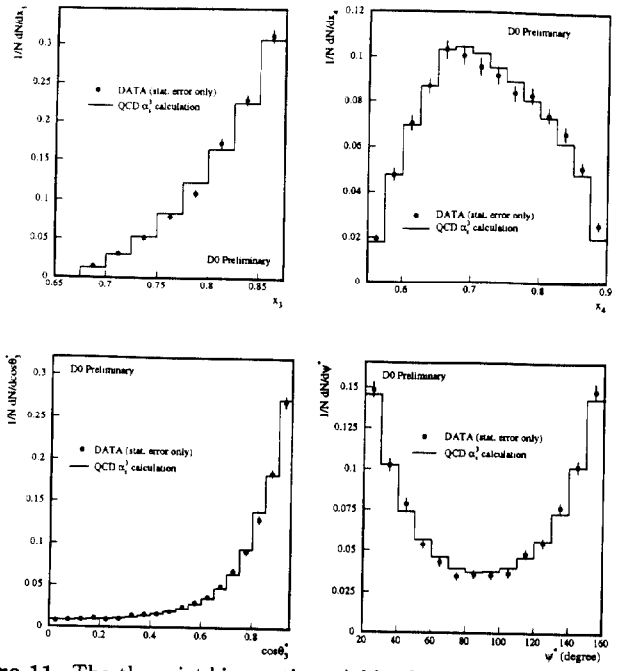

Figure 11. The three-jet kinematic variables for D0 measured at lower m_{3j}.

5. Acknowledgements

Thanks to John Womersley for providing me with the D0 photon plots and to Jerry Blazey for the D0 three-jet plots.

References

[1] H. Baer, J. Ohnemus and J.F. Owens, Phys. Lett. **B234** (1990) 127.
[2] CDF Collaboration: F. Abe *et al.*, Phys. Rev. **D45** (1992) 2249.
[3] W. Giele, private communication.
[4] A. Martin, R. Roberts and W. Stirling, Phys. Lett. **B309** (1993) 492.
[5] G. Marchesini and B. Webber,Nucl. Phys. **B310** (1988) 461.
[6] CTEQ Collaboration: J. Botts *et al.*, Phys. Lett. **B304** (1993) 159.
[7] W. Giele *et al.*, Snowmass Summer Study 1990, p.137.
[8] UA1 Collaboration: G. Arnison *et al.*, Phys. Lett. **B158** (1985) 494;
CDFCollaboration: F. Abe *et al.*, Phys. Rev. **D45** (1992) 1448